

Supplementary Information

Long-Term Distribution Patterns of Chlorophyll-a Concentration in China's Largest Freshwater Lake: MERIS Full-Resolution Observations with a Practical Approach. *Remote Sens.* 2014, 1, 275–299

Lian Feng ^{1,2,3}, Chuanmin Hu ², Xingxing Han ¹, Xiaoling Chen ^{1,3,*} and Lin Qi ^{2,4}

¹ State Key Laboratory of Information Engineering in Surveying, Mapping and Remote Sensing, Wuhan University, Wuhan 430079, China; E-Mails: lian.feng@whu.edu.cn (L.F.); xxhan1989@gmail.com (X.H.)

² College of Marine Science, University of South Florida, 140 Seventh Avenue South, St. Petersburg, FL 33701, USA; E-Mails: huc@usf.edu (C.H.); lqi@mail.usf.edu (L.Q.)

³ Collaborative Innovation Center for Geospatial Information Technology, Wuhan University, Wuhan 430079, China

⁴ State Key Laboratory of Lake Science and Environment, Nanjing Institute of Geography and Limnology, Chinese Academy of Sciences, Nanjing 210008, China

* Author to whom correspondence should be addressed; E-Mail: xiaoling_chen@whu.edu.cn; Tel.: +86-27-6877-9233.

Atmospheric correction of satellite ocean color measurements over turbid lakes has been problematic due to a number of reasons, and this problem is particularly severe for lakes in East China because of significant aerosol perturbations and complex in-water optical properties. Currently, for MERIS measurements there is *no* atmospheric correction that works well for Poyang Lake or other lakes in East China. Several popular algorithms and software packages were attempted in order to derive reasonable R_{rs} data from the MERIS measurements, and they all showed unsatisfactory results. These included both NASA's software SeaDAS and ESA's software BEAM. The standard atmospheric correction algorithm embedded in SeaDAS (version 6.4) often masked many water pixels, and for non-masked water pixels the algorithm frequently resulted in negative R_{rs} values. Likewise, atmospheric correction in the "Lake Module" and "Neural Network Module" of the BEAM software did not work well either—even the derived R_{rs} spectral shape was not correct, not to mention the magnitude.

Figure S1 shows the BEAM-retrieved R_{rs} from Taihu Lake (another turbid lake in China), as compared with the field-measured R_{rs} and Rayleigh-corrected R_{rc} . Neither the magnitude nor the spectral shape in the BEAM-retrieved R_{rs} appeared correct. For locations #1 and #2, the 560-nm *in situ* R_{rs} peak shifted to 620 nm in the BEAM-retrieved R_{rs} . For location #3 from the intense bloom, the magnitude of the BEAM-retrieved R_{rs} was much lower than the field-measured R_{rs} , and the enhanced reflectance in the near-infrared completely disappeared in the BEAM-derived R_{rs} . In contrast, the spectral shapes of all three

locations in the Rayleigh-corrected reflectance (R_{rc} , right panel in Figure S1) can all find their counterparts in the field-measured R_{rs} , and their magnitudes (after dividing by π to convert to Rayleigh-corrected R_{rs}) are only slightly higher than the field-measured R_{rs} due to aerosol scattering. In short, Rayleigh corrected R_{rc} data appeared much more reasonable in both the spectral shape and reflectance magnitude than the fully corrected R_{rs} for this turbid lake.

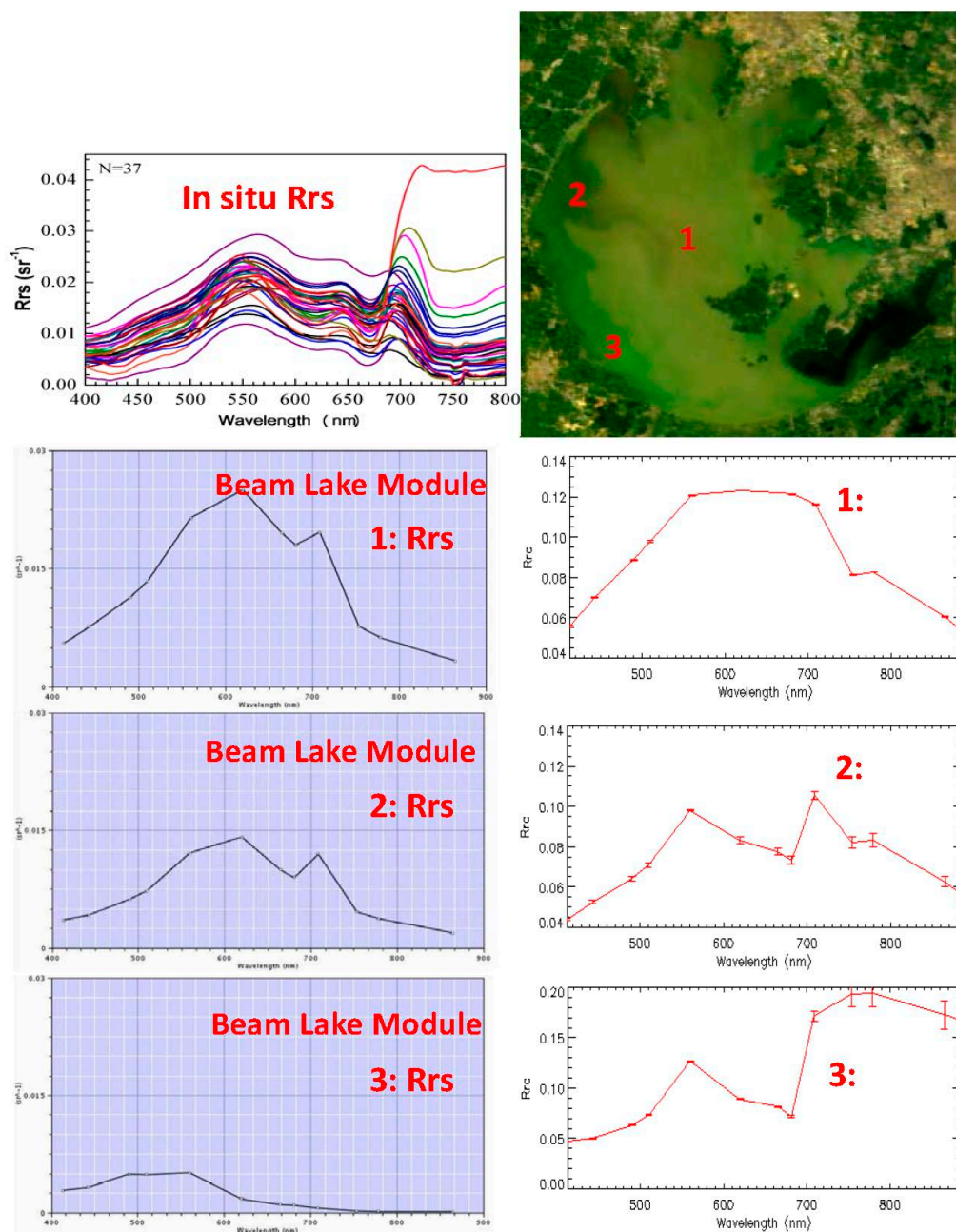


Figure S1. Justification of using partially corrected MERIS R_{rc} data instead of the fully corrected MERIS R_{rs} data (using BEAM's turbid-water atmospheric correction module). Reflectance data were extracted from three locations (1–3), representing sediment-rich non-bloom water, moderate bloom, and intense bloom, respectively. The BEAM-derived spectral R_{rs} are shown in the left panels, while the field-measured R_{rs} (all data) and Rayleigh-corrected R_{rc} are shown in the right panels.

Figure S2 shows similar findings for Poyang Lake. Lower-than-real R_{rs} was derived from the BEAM software. Consequently, Chl-a distribution patterns from the BEAM NN module (middle and right panels in Figure S3) did not appear correct. High Chl-a was observed in the red circled regions, which appeared unrealistic as Chl-a in these regions should appear relatively homogeneous due to lack of non-point nutrient sources. In addition, the magnitudes of Chl-a from the BEAM processing for the entire lake also appeared unrealistically high. In contrast, the NRGDI algorithm (with MERIS R_{rc} as input) yielded reasonable spatial patterns of Chl-a (left panel of Figure S3) whose magnitude also agreed qualitatively with field-determined Chl-a.

These observations are consistent with those shown in Figures 12 and 13 of this manuscript, indicating the shortcoming of the BEAM software (and its embedded algorithms). The exact reason of these algorithm artifacts was unknown, but could possibly be due to the fact that the BEAM plug-in modules were primarily developed for European waters where optical constraints used in the iterative atmospheric correction could be drastically different from those for Chinese lakes. These results did not imply that NRGDI was superior to other popular algorithms, but simply indicated that other algorithms did not work well for Poyang Lake, possibly due to its different optical properties than those used in developing the other algorithms. Nevertheless, before a validated atmospheric correction approach is developed, alternative ways must be sought to derive the surface reflectance from MERIS measurements. This is exactly why partially corrected MERIS data (*i.e.*, Rayleigh-corrected reflectance, R_{rc}) was used in this study to derive Chl-a with the NRGDI algorithm, whose sensitivity to aerosol perturbations was thoroughly investigated and presented in the manuscript.

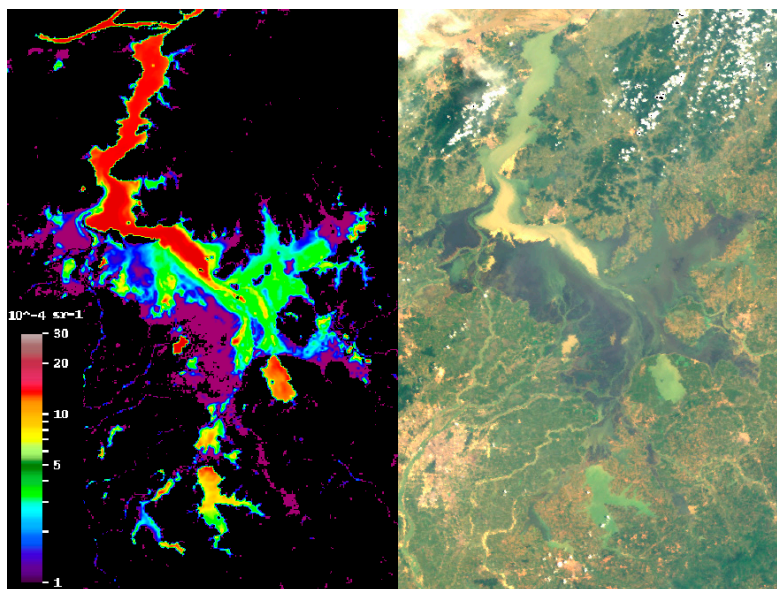


Figure S2. Left: RGB composite of MERIS image on 5 July 2011; Right: $R_{rs}(865)$ derived from the BEAM Neural Network plug-in module. Although a direct validation using concurrent field data was not available, the $R_{rs}(865)$ values appeared much smaller than the *in situ* $R_{rs}(865)$ measured from other times for TSS > 10 mg/L.

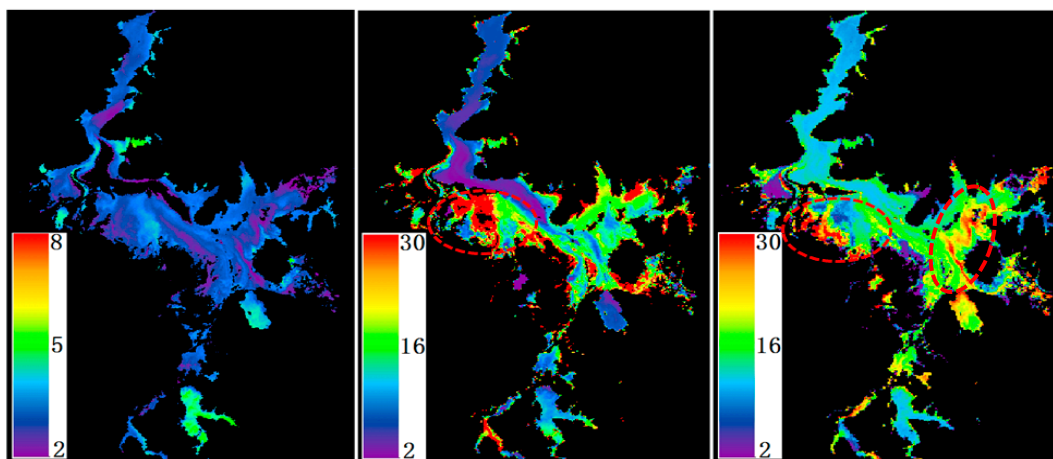


Figure S3. Chl-a maps derived from MERIS data (5 July 2011) using different methods. **Left:** NRGDI algorithm with R_{rc} as inputs; **Middle:** NRGDI algorithm using BEAM R_{rs} (NN plug-in module) as inputs; **Right:** Direct product of the BEAM NN module.

© 2014 by the authors; licensee MDPI, Basel, Switzerland. This article is an open access article distributed under the terms and conditions of the Creative Commons Attribution license (<http://creativecommons.org/licenses/by/4.0/>)